Synthesis and Mechanical Performance of Biological-like Hydroxyapatites

S. Kannan, A. F. Lemos, and J. M. F. Ferreira*

Department of Ceramics and Glass Engineering, University of Aveiro, CICECO, 3810-193 Aveiro, Portugal

Received November 21, 2005. Revised Manuscript Received February 28, 2006

Synthesis of hydroxyapatites (HAP) with cosubstituted essential trace elements (Na, Mg, K, Cl, and F) of natural bone was performed through aqueous precipitation. The powders were characterized using elemental analysis, X-ray diffraction, and Fourier transform infrared spectroscopy. The results obtained proved that substituted elements play a crucial role in enhancing the thermal stability of the HAP phase until 1400 °C, when compared to the stoichiometric HAP which decomposed to α-tricalcium phosphate beyond 1200 °C. A noticeable amount of β-TCP along with the HAP phase has also been detected after calcination at higher temperatures, which tended to increase with increasing the incorporation levels of trace elements. Significant improvements in the mechanical properties were obtained for sintered specimens of the cosubstituted hydroxyapatites in comparison to pure HAP.

1. Introduction

Synthetic hydroxyapatite (HAP) is the most ubiquitous family of calcium phosphates that are well-known for their use in biological applications. The similarity of the crystallographic structure of natural bone, enamel, and dentin to that of synthetic HAP, along with the chemical analyses showing the presence of calcium and phosphate as principal constituents in these minerals, led to the belief that the inorganic components of bone and teeth are essentially calcium HAP represented by the chemical formula $Ca_{10}(PO_4)_6(OH)_2$.[1−4] In spite of the structural and crystallographic similarities with synthetic HAP, the biological apatites are always nonstoichiometric with structural imperfections due to several incorporated elements on trace levels in its lattice.[5−7] Although these elements are embedded in trace levels in the composition of biological apatites, several studies proved their determining role on the biological process upon implantation.[8−18] Some of the salient features of these trace elements are described as follows to have a thorough understanding: (a) sodium, a monovalent ion, available in abundance next to calcium and phosphorus, which plays a significant role on bone metabolism and osteoporosis;[8,9] (b) magnesium, undoubtedly one of the most important bivalent ions associated with the biological apatite, which has its own significance in the calcification process, bone fragility, and its indirect influence on mineral metabolism;[10−12] (c) potassium, active in mineralization and biochemical processes;[13,14] (d) fluorine, well-recognized for its potential behavior on the stability of apatite and its prevention in dental caries;[15,16] and (e) chlorine, which enables an acidic environment to develop on the surface of bone that activates osteoclasts in the bone resorption process.[17,18] As a result of the significant roles played by these trace elements in the biological process, nowadays numerous studies have been undertaken aiming at the synthesis of ionic substituted HAP either with single elements[19−27] or with coupled element substitutions.[29−33]

* Corresponding author. Tel.: +351-234-370242. Fax: +351-234-425300. E-mail: jmf@cv.ua.pt.

(1) Hench, L. L. *J. Am. Ceram. Soc.* **1991**, *74*, 1487−1510.
(2) Aoki, H. *Science and medical applications of hydroxyapatite*; JAAS: Tokyo, Japan, 1991.
(3) Jarcho, M.; Bolen, C. H.; Thomas, M. B.; Bobick, J.; Kay, F.; Doremus, R. H. *J. Mater. Sci.* **1976**, *11*, 2027−2035.
(4) Le Geros, R. Z.; Le Geros, J. P. *Dense hydroxyapatite, An introduction to bioceramics*; World Scientific: Singapore, 1993.
(5) LeGeros, R. Z. *Calcium phosphates in oral biology and medicine*; Karger AG Publishers: Basel, Switzerland, 1991.
(6) Rey, C. *Calcium phosphates for medical applications*; Kluwer Academic Publishers: Boston, 1998; pp 217−239.
(7) Elliott, J. C. *Structure and chemistry of the apatites and other calcium orthophosphates*; Elsevier: Amsterdam, 1994.
(8) Itoh, R.; Suyama, Y. *Am. J. Clin. Nutr.* **1996**, *63*, 735−740.
(9) Ginty, F.; Flynm, A.; Cashman, K. D. *Br. J. Nutr.* **1998**, *79*, 343−350.
(10) Bigi, A.; Foresti, E.; Gregoriani, R.; Ripamonti, A.; Roveri, N.; Shah, J. S. *Calcif. Tissue Int.* **1992**, *50*, 439−444.
(11) Althoff, J.; Quint, P.; Krefting, E. R.; Hohling, H. J. *Histochemistry* **1982**, *74*, 541−552.
(12) Martini, L. A. *Nutr. Rev.* **1999**, *57*, 227−229.
(13) Wiesmann, H. P.; Plate, U.; Zierold, K.; Hohling, H. J. *J. Dent. Res.* **1998**, *77*, 1654−1657.
(14) Krefting, E. R.; Lissner, L.; Hohling, H. J. *J. Phys.* **1984**, *45*, 465−468.
(15) Ten Cate, J. M.; Featherstone, J. D. B. *Crit. Rev. Oral Biol. Med.* **1991**, *2*, 283−296.
(16) Caverzasio, J.; Palmer, G.; Bonjour, J. P. *Bone* **1998**, *22*, 585−589.
(17) Schlesinger, P. H.; Blair, H. C.; Teitalbaum, S. L.; Edwards, J. C. *J. Biol. Chem.* **1997**, *272*, 18636−18643.
(18) Neuman, W. F.; Neuman, M. W. *The chemical dynamics of bone mineral*; University of Chicago Press: Chicago, 1958.
(19) Yang, Z.; Jiang, Y.; Yu, L.; Li, F.; Sun, S.; Hou, T. *J. Mater. Chem.* **2005**, *15*, 1807−1811.
(20) Kannan, S.; Lemos, I. A. F.; Rocha, J. H. G.; Ferreira, J. M. F. *J. Solid State Chem.* **2005**, *178*, 3190−3196.
(21) Suchanek, W. L.; Byrappa, K.; Shuk, P.; Riman, R. E.; Janas, V. F.; Ten Huisen, K. S. *Biomaterials* **2004**, *25*, 4647−4657.
(22) Rodríguez-Lorenzo, L. M.; Hart, J. N.; Gross, K. A. *Biomaterials* **2003**, *24*, 3777−3785.
(23) Kannan, S.; Ventura, J. M.; Ferreira, J. M. F. *Chem. Mater.* **2005**, *17*, 3065−3068.
(24) Gross, K. A.; Rodríguez-Lorenzo, L. M. *Biomaterials* **2004**, *25*, 1375−1384.

10.1021/cm052567q CCC: $33.50
Published on Web 03/22/2006

Because the hierarchical structure of apatite has the ability to accept a wide number of possible substitutions in its lattice,[34] the job was considered to be easier in substituting the elements in trace levels. However, to date there is no evidence of specific documentation on the combined substitution of all the elements in the HAP structure, which will be certainly a better behaved material in the biological action course upon implantation. In view of this perspective, the aims of the present work are (i) to prepare synthetic HAP with combined substituted biocompatible trace elements present in biological apatite and (ii) to improve the thermal stability of the HAP phase and enhance densification at high temperatures to get mechanically stronger materials. The synthesis was performed on the bulk scale to ensure the reproducibility of the experimental results.

2. Materials and Methods

2.1. Preparation. The synthesis in bulk was carried out in a fully automated apparatus (capacity = 6 L) with a specific device to control the stirring of the suspensions, the addition rate of the reactants, and the temperature of the system. Calcium nitrate tetrahydrate [$Ca(NO_3)_2 \cdot 4H_2O$, Vaz-Pereria-Portugal], diammonium hydrogen phosphate [$(NH_4)_2HPO_4$, Vaz-Pereria-Portugal], sodium nitrate [$NaNO_3$, Vaz-Pereria-Portugal], magnesium nitrate hexahydrate [$Mg(NO_3)_2 \cdot 6H_2O$, Merck], potassium nitrate [KNO_3, Merck], ammonium chloride [NH_4Cl, Merck], and ammonium fluoride [NH_4F, Merck] were used as starting chemical precursors for the synthesis. Two different types of compositions were attempted to form HAP with cosubstituted elements. With this purpose, a mixture of $(NH_4)_2HPO_4$, NH_4F, and NH_4Cl solutions was added slowly at a rate of 50 mL/min to the solution mixture containing nitrates of Ca, Na, Mg, and K stirred at a rate of 1000 rpm (solution concentrations of precursors detailed in Table 1). After the addition of all the precursors, the pH value of the mixture was found to be around 4. The pH of the mixed solution was then increased to 10 by adding concentrated ammonium hydroxide (NH_4OH) solution. After the completion of addition, the reaction was performed at 90 °C for 2 h under a constant stirring rate of 1000 rpm. A pure stoichiometric HAP without any additives was prepared under the same conditions to compare the results. The precipitated suspension was poured out from the reactor and allowed to settle down for 24 h for the maturation of the precipitate. After 24 h, the precipitates were separated through vacuum filtration and dried at 80 °C overnight. The precipitates were washed and filtered repeatedly with deionized water. The dried cakes were ground to fine powders, sieved through a mesh size of 200 μm, and used for characterization studies.

Table 1. Concentrations of the Precursors Used in Synthesis of HAP with Substituted Elements

	S-HAP1		S-HAP2	
precursor	molarity	weight (g) of the precursors in 2000 mL	molarity	weight (g) of the precursors in 2000 mL
$Ca(NO_3)_2 \cdot 4H_2O$	2.0	944.40	2.0	944.40
$(NH_4)_2HPO_4$	1.2	316.94	1.2	316.94
$NaNO_3$	0.1	16.99	0.05	8.498
$Mg(NO_3)_2 \cdot 6H_2O$	0.08	41.01	0.04	20.51
KNO_3	0.06	12.13	0.03	6.07
NH_4Cl	0.1	10.69	0.05	5.35
NH_4F	0.1	7.408	0.05	3.70
Ca/P ratio	1.67		1.67	
(Ca + Na + Mg + K)/P ratio	1.86		1.76	

2.2. Characterization. X-ray diffraction (XRD) studies on both as-prepared and calcined powders were carried out using a high-resolution Rigaku Geigerflex D/Mac, C Series diffractometer with Cu Kα radiation ($\lambda = 1.5406$ nm) produced at 30 kV and 25 mA, and the diffraction angles (2θ) were scanned between 20° and 50° with a step size of 0.02° 2θ/s. Calcination was carried out in a Thermolab furnace (Pt30%Rh/Pt6%Rh thermocouple) with a heating rate of 5 °C/min to achieve a predetermined temperature range and a dwell time of 2 h which was again cooled to room temperature at the rate of 5 °C/min. Lattice constants were determined by least-squares refinements from the well-determined positions of the most intense reflections that were processed by MDI Jade 6.1 software. For this purpose, the reflection planes (002), (211), (112), (300), (222), and (213) for the HAP phase were used for the calculation. The volume V of the hexagonal unit cell was determined for each HAP formulation from the relation $V = 2.589a^2c$. Quantitative determination of the phase compositions of biphasic mixtures were made using X'Pert High Score 1.0 *f*, PANalytical B.V, using the International Center for Diffraction Data (2004) database.

The sizes of individual HA crystallites were calculated from XRD data using the Scherrer approximation.[35] The values of full width at half-maximum intensity ($h_{1/2}$) of the peak of the (002) plane, representative of the crystallites along the c axis, and of the peak of the (300) plane, representative of the crystallites along the a axis, were used in the calculation according to eq 1

$$d = K\lambda/h_{1/2} \cos\theta \quad (1)$$

where d is the crystallite size, as calculated for the (hkl) reflection, λ is the wavelength of Cu Kα radiation (0.154 06 nm), and k is the broadening constant varying with crystal habit and chosen as 0.9 for the elongated apatite crystallites.[36]

Elemental analyses for the presence of all elements except fluorine were made using X-ray fluorescence spectroscopy (Philips PW2400 X-ray fluorescence spectrometer). The vacuum of the chamber was lower than 2 Pa. The error associated to each chemical element could be determined as ±1 of the last digit (Table 2) of the measured values. Fluorine was determined by the selective ion electrode method. Infrared spectra for the powders were obtained using an Fourier transform infrared (FT-IR) spectrometer (model Mattson Galaxy S-7000, U.S.A.). For this purpose each powder

(25) Lin, F. H.; Liao, C. J.; Chen, K. S.; Sun, J. S. *Biomaterials* **1998**, *18*, 1101−1107.
(26) Suchanek, W.; Yashima, M.; Kakihana, M.; Yoshimura, M. *Biomaterials* **1998**, *18*, 923−933.
(27) Yanagisawa, K.; Rendon-Angeles, J. C.; Ishizawa, N.; Oishi, S. *Am. Mineral.* **1999**, *84*, 1861−1869.
(28) Bertoni, E.; Bigi, A.; Cojazzi, G.; Gandolfi, M.; Panzavolta, S.; Roveri, N. *J. Inorg. Biochem.* **1998**, *72*, 29−35.
(29) Mayer, I.; Schlam, R.; Featherstone, J. D. B. *J. Inorg. Biochem.* **1997**, *66*, 1−6.
(30) Feki, H. El.; Amami, M.; Ben Salah, A.; Jemal, M. *Phys. Status Solidi* **2004**, *1*, 1985−1988.
(31) De Maeyer, E. A. P.; Verbeeck, R. M. H.; Naessens, D. E. *Inorg. Chem.* **1993**, *32*, 5709−5714.
(32) Yamasaki, Y.; Yoshida, Y.; Okazaki, M.; Shimazu, A.; Uchida, T.; Kubo, T.; Akagawa, Y.; Hamada, Y.; Takahashi, J.; Matsuura, N. *J. Biomed. Mater. Res.* **2002**, *62*, 99−105.
(33) Gibson, I. R.; Bonfield, W. *J. Mater. Sci.: Mater. Med.* **2002**, *13*, 685−693.
(34) Cazalbou, S.; Combes, C.; Eichert, D.; Rey, C. *J. Mater. Chem.* **2004**, *14*, 2148−2153.
(35) Cullity, B. D. *Elements of X-ray Diffraction*; Addison-Wesley: Reading, MA, 1978.
(36) Klug, H. P.; Alexander, L. E. *X-ray Diffraction Procedures*; Wiley: New York, 1959.

Table 2. Concentrations of the Elements Measured in HAP after Heat Treatment [HAP = 1200 °C, S-HAP1 and S-HAP2 = 1400 °C]

	concentration of the element (wt %)						
sample	Ca	P	Na	Mg	K	F	Cl
bone[2,4]	24.5	11.5	0.7	0.55	0.03	0.02	0.1
enamel[2,4]	36.0	17.7	0.5	0.44	0.08	0.01	0.3
HAP	39.89	18.50	~0.02	~0.01			
S-HAP1	39.31	18.32	1.11	0.94	1.09	0.09	0.06
S-HAP2	38.99	18.17	0.493	0.51	0.47	0.04	0.03

was mixed with KBr in the proportion of 1/150 (by weight) for 15 min and pressed into a pellet using a hand press.

2.3. Mechanical Tests. The as-prepared powders were calcined at 1100 °C and then dry milled for 30 min in a high-speed porcelain mill, resulting in mean particle sizes around 1.5 μm for all the powders (measured in a particle size analyzer COULTER LS230, U.K., with a Fraunhofer optical model). A stock suspension of each powder was prepared with 55 vol % solids loading and stabilized using 1.5 wt % Targon 1128 (BK Ladenburg, Germany), according to a procedure previously described.[37] To obtain good compaction during pressing, 3 wt % of Mowilith DM 2 HB (Clariant, Spain) and 1.5 wt % of PEG200 (Aldrich, Germany, based on the dry mass of solids) were added to suspensions as respectively the binder and plasticizer, and the mixtures were left to homogenize for 1 h in a rolling system. The as-prepared suspensions were then granulated by freeze granulation (PowerPro freeze granulator LS-2, Sweden), and the granules were dried in a freeze-dry system (Labconco, LYPH Lock 4.5) for 72 h. After complete drying, the granules were pressed in rectangular bars with 4 mm × 5 mm × 50 mm by uniaxial pressing (80 MPa). After debinding at 550 °C for 2 h, the bars were sintered at different temperatures, according to the phase stability, for 2 h at a heating rate of 5 °C/min.

Flexural strength was measured in series of 20 specimens using a three-point bending device and Shimadzu equipment (Shimadzu Autograph AG-IS, 10 kN, Kyoto, Japan), at a *crosshead speed* of 0.5 mm/min. For all the samples, the load-displacement curves presented an elastic region ending with brittle fracture.

Vickers hardness tests were carried out using a Zwick/Roell hardness tester (Zwick/Roell ZHU, Ulm, Germany). Polished samples were indented with a Vickers diamond pyramidal indenter having a square base and 136° pyramidal angles. The load was 5 kg, 20 indentations were made, and the averaged hardness values were taken for the analysis.

Microstructure observations made at the etched surfaces of the sintered bars (immersion in 15% H_3PO_4 solution for 15 s) were done by scanning electron microscopy (SEM; Hitachi, S-4100, Tokyo, Japan, 25 kV acceleration voltage, beam current 10 μA). The density of the sintered samples was determined by the Archimedes method by immersion in mercury.

3. Results and Discussion

3.1. As-Prepared Powders. The XRD patterns of the as-prepared powders are presented in Figure 1. All the powders indicate the formation of apatite differing only in peak width and absolute intensity of the diffraction patterns. The substitution of all elements did not appear to significantly affect the diffraction pattern of the as-prepared powder. It should be noted that XRD analysis of as-precipitated apatite powders resulted in diffraction patterns that could resemble HAP even though the Ca/P ratio was greater or less than

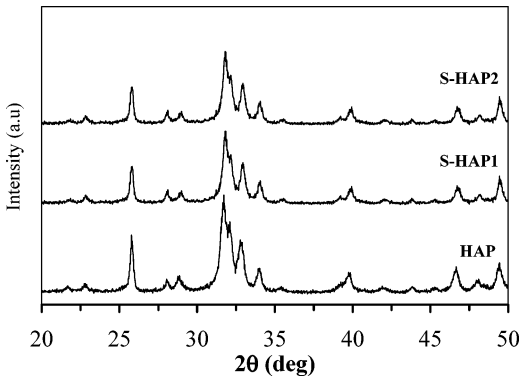

Figure 1. XRD patterns for the as-prepared powders.

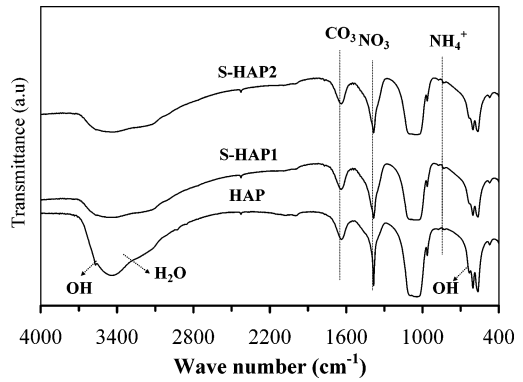

Figure 2. FT-IR spectra for the as-prepared powders.

the stoichiometric molar ratio of 1.67 for HAP.[38,39] FT-IR spectra displayed in Figure 2 also confirm that apatite formed in all the powders with the observed fundamental vibrational modes of PO_4 group at 475, 574, 609, 966, and 1020−1120 cm^{-1}. The bands corresponding to OH group of the HAP phase can be witnessed at 630 and 3570 cm^{-1} for stoichiometric HAP but are not clearly visible for S-HAP1 and S-HAP2 that contain the substituted elements. However, it is difficult to explain the role of substituted elements in the structure of the as-prepared powders considering the poor crystallinity of the phases formed, requiring heat treatment to improve the crystallinity for a more precise characterization.

Other relevant information from the FT-IR spectra is the presence of the adsorbed water that could also be detected in the region around 3300−3600 cm^{-1}. The CO_3 detected in the FT-IR spectra of as-prepared powders in the region around 1650 cm^{-1} is due to the adsorbed species remaining from the aqueous precipitation. The presence of nitrates (NO_3) in the as-dried powders is obvious from the peaks witnessed in the FT-IR patterns in the region around 1320−1480 cm^{-1}. The presence of residual NH_4^+ ions at 875 cm^{-1} and nitrates is apparent in all the as-prepared powders, which tends to coincide with the observations made in a previous study.[40]

3.2. Calcined Powders. *3.2.1. Elemental Analysis.* The elemental analyses of the calcined powders are presented in

(37) Lemos, A. F.; Santos, J. D.; Ferreira, J. M. F. *Adv. Mater. Forum* **2004**, *361*, 455−456.

(38) Gibson, I. R.; Rehman, I.; Best, S. M.; Bonfield, W. *J. Mater. Sci.: Mater. Med.* **2000**, *12*, 799−804.

(39) Gibson, I. R.; Best, S. M.; Bonfield, W. *J. Biomed. Mater. Res.* **1999**, *44*, 422−428.

(40) Raynaud, S.; Champion, E.; Bernache-Assollant, D.; Thomas, P. *Biomaterials* **2002**, *23*, 1065−1072.

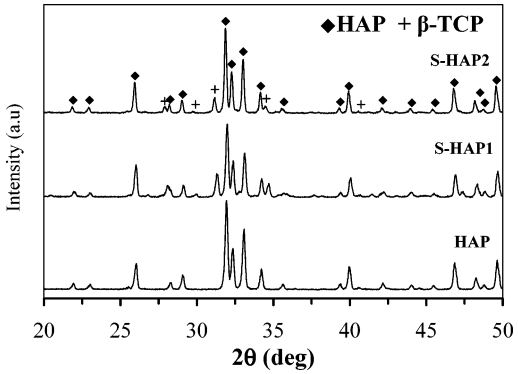

Figure 3. XRD patterns for the apatite powders after calcination [HAP = 1200 °C, S-HAP1 and S-HAP2 = 1400 °C].

the Table 2. From these data one can conclude that the expected Ca/P molar ratio has been achieved for the HAP powder, while slightly smaller values (Ca/P ~ 1.66) were measured for S-HAP1 and S-HAP2. Regarding all the substituted elements, a good correlation can be observed between the elemental analysis of calcined S-HAP1 and S-HAP2 powders and the added concentration of each element during the synthesis. Accordingly, higher levels of incorporated elements are detected in S-HAP1 in comparison to the S-HAP2 that shows more or less half the value of S-HAP1. It is also reasonable to mention that the natural bone and tooth mineral consists of all these elements, but the composition may vary depending upon the age, sex, and nature of the species.[41,42] Hence, it is obvious that this synthesis method can be effective in achieving the desired concentration of substituted elements by varying the concentration of the precursors added during the synthesis.

3.2.2. X-ray Diffraction. The XRD patterns for HAP (1200 °C), S-HAP1, and S-HAP2 (1400 °C) are presented in Figure 3. All the patterns confirm the formation of HAP of better crystallinity by the observed sharp diffraction patterns when compared to the patterns of as-prepared powders. It is apparent from the X-ray patterns that calcination at higher temperature has led to the formation of the β-TCP phase along with the HAP for the samples S-HAP1 and S-HAP2. The amounts of β-TCP were 34% for the S-HAP1 powder containing higher concentration of the substituted elements and 22% for the S-HAP2 powder that possesses comparatively lower levels of substituted elements. This proves that cosubstitution of all the elements had tremendous impact on the formation of β-TCP along with the HAP. Moreover, the content of β-TCP formed upon heat treatment at high temperature is dependent on the concentration of the added elements. These results are in good accordance with the previous studies reported by the authors showing that even though the stoichiometric Ca/P molar ratio of 1.67 was used, essential for the formation of pure HAP, the substituted elements in the apatite lattice can lead to formation of β-TCP upon calcination beyond 1000 °C.[43,44] The calculated lattice parameters for S-HAP1 and S-HAP2 (Table 3) samples also

Table 3. Calculated Lattice Constant Values after Calcination[a]

	lattice constant (Å)			crystallite size (nm)	
sample	*a* axis (±0.0004)	*c* axis (±0.0004)	volume (±0.03)	X_{002}	X_{300}
ICDD no. 09-432	9.418	6.884	1580.84		
HAP	9.4087	6.8489	1571.35	38.2 ± 2.2	41.2 ± 3.6
S-HAP1	9.3975	6.8432	1564.64	49.6 ± 3.4	64.2 ± 3.2
S-HAP2	9.4023	6.8640	1571.01	48.2 ± 2.8	61.7 ± 2.8

[a] For HAP, the parameters were calculated at 1200 °C, and for S-HAP1 and S-HAP2, the parameters were calculated at 1400 °C.

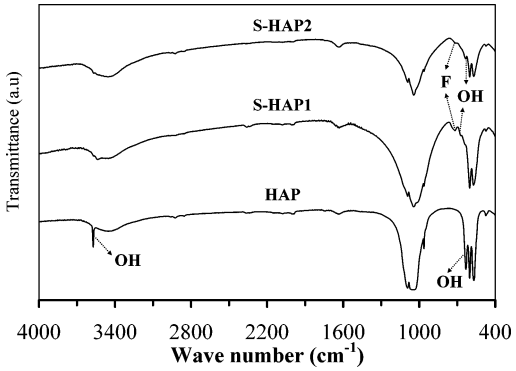

Figure 4. FT-IR spectra for the apatite powders after calcination [HAP = 1200 °C, S-HAP1 and S-HAP2 = 1400 °C].

confirm the formation of a hexagonal apatite system with minor differences in comparison to the stoichiometric HAP, which are solely due to the role of incorporated elements in the apatite lattice. The significance of the present results is the excellent thermal stability exhibited by resultant S-HAP1 and S-HAP2 powders, which did not decompose to the undesirable α-TCP phase until 1400 °C, contrary to the pure stoichiometric HAP that decomposed to α-TCP after calcination at 1300 °C.[43,44] In the case of substituted apatites, S-HAP1 and S-HAP2, only the desirable β-TCP phase has been detected along with the HAP phase even after calcination at 1400 °C. The crystallite size values obtained from the (002) plane [termed X_{002}] and (300) plane [termed X_{300}] are presented in Table 3. The crystallite size measured from X_{002} corresponds for the *c* axis, whereas the values measured from X_{300} correspond to the *a* axis. It is well seen from the Table 3 that the calculated values are around 50 nm size for all the powders, thus having excellent coincidence with that of bone mineral crystallite size.[45,46]

3.2.3. Role of Substituted Elements. In the case of synthetic HAP with substituted elements, the existing scientific reports have well-documented the behavior of single or coupled element substitution in the apatite lattice. The incorporation of foreign ions in the synthetic HAP can induce subtle changes in the resultant crystallographic parameters depending upon its concentration and nature of the additives, and the most critical is its size. Regarding Na (0.97 Å), its incorporation is facilitated depending on the nature of the precursors.[26] With certain additives, it has been proved that Na incorporation favors the formation of pure HAP whereas

(41) Le Geros, R. Z.; Balmain, N.; Bonel, G. *Calcif. Tissue Res.* **1987**, *41*, 137.
(42) Handschin, R. G.; Stern, W. B. *Clin. Rheumatol.* **1994**, *13*, 75.
(43) Kannan, S.; Rocha, J. H. G.; Ferreira, J. M. F. *J. Mater. Chem* **2006**, *3*, 286−291.
(44) Kannan, S.; Ferreira, J. M. F. *Chem. Mater.* **2006**, *18*, 198−203.
(45) Danilchenko, S. N.; Kukharenkoi, O. G.; Moseke, C.; Protsenko, I. Y.; Sukhodubi, L. F.; Sulkio-cleff, B. *Cryst. Res. Technol.* **2002**, *37*, 1234.
(46) Kinney, J. H.; Pople, J. A.; Marshall, G. W.; Marshall, S. J. *Calcif. Tissue Int.* **2001**, *69*, 31.

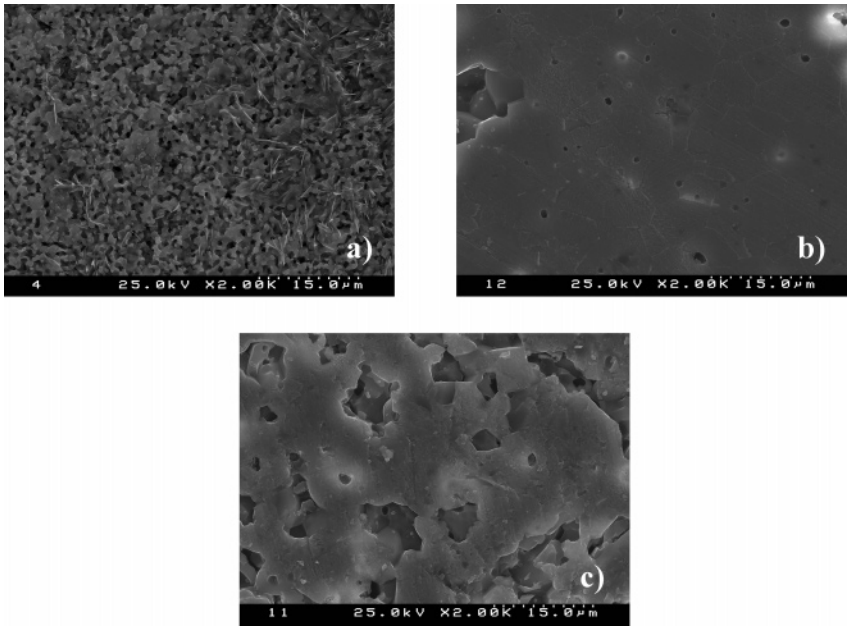

Figure 5. SEM micrographs for the etched surface of sintered HAPs: (a) HAP sintered at 1200 °C; (b) S-HAP1 sintered at 1400 °C; (c) S-HAP2 sintered at 1400 °C.

in certain cases trace levels of β-tricalcium phosphate (β-TCP) and calcium oxide (CaO) have been detected in the resultant powder after heat treatment. In the case of Mg, its stabilization role on the β-TCP phase upon heat treatment above 800 °C has been well-recognized.[20,21] There are reports on its significant influence on the lattice constant values due to size mismatch with Ca (Ca, 0.99 Å; Mg, 0.66 Å). Potassium (1.33 Å) has a bigger size than Ca and, hence its incorporation into the apatite structure can favor significant variations in the resultant lattice values. There is also evidence about the combined substitution of Mg and CO_3 as well as Na and CO_3 into the apatite structure that can result in the formation of the pure HAP phase while heating in careful consideration of preserving volatile CO_3 at high temperatures.[31,33] In the case of anionic substitutions of both Cl (1.81 Å) and F (1.36 Å), the prevailing reports strongly suggest their replacement for OH groups while incorporation into the apatite structure, thus causing expansion or contraction of lattice constants. Some studies have indicated that partial replacement of F for the OH group can cause the formation of a trace level of the β-TCP phase upon heat treatment.[22] The effect of a single or a couple of substitutions on the apatite structure can be understood from the existing reports. However, the incorporation of all these elements in the apatite is more complex and has never been reported before. The present results show that the structure of the apatite phase has been preserved except for some small observed discrepancies in the lattice values. Hence the statement that "hierarchical structure of apatite is ready to accept a wide variety of ionic substitutions (both cationic and anionic) with no significant changes in the hexagonal apatite structure"[34] is proved from the present results.

3.2.4. FT-IR Spectra. FT-IR patterns presented in Figure 4 also confirm the formation of the apatite phase for the S-HAP1 and S-HAP2 powders. Bands respective of PO_4 tetrahedra are visible at 475 cm^{-1} (O−P−O bending υ_2), 576 cm^{-1} (O−P−O antisymmetric bending υ_4), 605 cm^{-1} (O−P−O bending υ_4), 975 cm^{-1} (P−O stretching υ_1), and 1086 cm^{-1} (P−O stretching υ_3). Interestingly, as a result of the incorporated F and Cl in the apatite structure, the bands for OH groups at 630 cm^{-1} (librational mode) and 3570 cm^{-1} (stretching frequency) are not clearly visible in the FT-IR spectra of both S-HAP1 and S-HAP2 as viewed in pure HAP. The characteristic feature of F has been witnessed at 725 cm^{-1},[23] whereas in the case of Cl no specific signal can be determined from the FT-IR spectra. In a previous study[47] the authors have reported that the incorporation of Cl in the apatite structure does not give any characteristic signal in the infrared region, except masking the bands for the OH group at both 630 and 3570 cm^{-1}. The different fluorine contents between the samples S-HAP1 and S-HAP2 can also be confirmed in the FT-IR spectra by the different intensities of the bands at 725 cm^{-1}. The most intense band is observed for the sample S-HAP1 containing a higher concentration of incorporated fluorine in comparison to the S-HAP2.

Table 4. Mechanical Test Data Obtained for the Sintered Bars after Pressing HAP (1200 °C), S-HAP1 (1400 °C), and S-HAP2 (1400 °C)

	mechanical data		
sample	flexural strength (MPa)	Vickers hardness HV5)	density (g/cm^3)
HAP	57.68 ± 15.36	297.45 ± 9.53	2.832 ± 0.051
S-HAP1	84.05 ± 7.93	376.21± 8.18	2.982 ± 0.0279
S-HAP2	63.95 ± 10.11	414.65 ± 8.91	2.935 ± 0.0297

3.2.5. Mechanical Properties. The data on the mechanical properties of HAP, S-HAP1, and S-HAP2 samples are presented in Table 4. It is apparent from Table 4 that the samples S-HAP1 and S-HAP2 have improved values of flexural strength, hardness, and density in comparison to those of the HAP sample.

The SEM micrographs of the etched surfaces of sintered samples HAP, S-HAP1, and S-HAP2 are presented in Figure

(47) Kannan, S.; Rocha, J. H. G.; Ferreira, J. M. F. *Mater. Lett.* **2006**, *60*, 864−868.

5. The microstructure of the less thermally stable HAP sample after sintering at 1200 °C is still significantly porous (Figure 5a) as a result of its poorer sintering behavior at this comparatively lower temperature that was used to avoid the decomposition of HAP into other phases such as α-TCP. On the Contrary, owing to the better thermal stability, the samples S-HAP1 (Figure 5b) and S-HAP2 (Figure 5c) could be sintered at 1400 °C, exhibiting dense microstructures. The higher thermal stability due to the substituted elements significantly improved the mechanical properties especially for the S-HAP1 sample that possesses higher concentration of substituted elements, exhibiting better mechanical properties toward S-HAP2.

4. Conclusions

The results presented and discussed in this work enable the following conclusions to be drawn:

(1) Synthetic HAPs with different levels of cosubstitution of all essential trace elements found in the biological apatite can be prepared.

(2) The synthesized cosubstituted apatite powders did not transform to the undesirable α-TCP until 1400 °C, giving rise to the formation of noticeable amounts of desirable β-TCP, depending on the substitution levels.

(3) The formation of resorbable β-TCP along with the nonresorbable HAP in the cosubstituted S-HAP1 and S-HAP2 certainly results in a better material for biomedical applications when compared to single or coupled element substituted HAP.

(4) The improved thermal stability of S-HAP1 and S-HAP2 favored densification and enhanced the mechanical properties in comparison to pure HAP.

(5) Although the exact position of the incorporated elements in the apatite structure cannot be determined from the present results, the method of synthesis proved that the essential biocompatible elements can be substituted in the synthetic apatite, without significant structural modifications.

Acknowledgment. Thanks are due to the Portuguese Foundation for Science and Technology for the financial support, Project No. POCTI/CTM/60207/2004, and for the fellowship grants of S.K. (SFRH/BPD/18737/2004) and A.F.L. (BD/8755/2002).

CM052567Q